Pergamon

Tetrahedron 56 (2000) 8703–8713

TETRAHEDRON

Cyclic Polylactones and their Cyclic Polyorthoester Valence Tautomers: Potential Ionophores

Ross P. McGeary[a,*] and Dorine N. Bruget[b]

[a]*Centre for Drug Design and Development, The University of Queensland, Brisbane, QLD 4072, Australia*
[b]*Department of Chemistry, The University of Queensland, Brisbane, QLD 4072, Australia*

Received 10 May 2000; revised 14 July 2000; accepted 10 August 2000

Abstract—The geometries and energies of the cyclic hexamer (**9**) of glycolic acid, and its polycyclic orthoester valence tautomer (**10**) have been studied by ab initio molecular orbital calculations at the HF/6-31G* and MP2//HF/6-31G* levels of theory. Both molecules are preorganised to bind metal ions in both endohedral and exohedral modes. The binding of **9** and **10** with Li^+, Na^+, K^+, Be^{2+}, Mg^{2+}, B^{3+} and Al^{3+} have been examined, and the energies and geometries of the resulting complexes are discussed.

Introduction

Ionophores are substances whose biological role is to transport metal ions across cell membranes. Neutral ionophores are often macrocycles that typically coordinate metal ions through oxygen atoms, either ether or carbonyl, and contain external hydrophobic groups to confer lipid solubility. Ionophores often have remarkable selectivity for particular metal ions. For example, nonactin (**1**) and tetranactin (**2**) are macrotetrolide antibiotics produced by various *Actinomyces* species, that coordinate the group IA metal ions and show high binding selectivity in the order $K^+ \sim Rb^+ > Cs^+ \gg Na^+$.[1] X-Ray crystal structures of nonactin complexed with K^+, Na^+, NH_4^+ and Cs^+, and of tetranactin complexed with Na^+, K^+, Rb^+, Cs^+ and NH_4^+, have been reported. All structures are very similar and show the cation coordinated by the four tetrahydrofuran ether oxygens and the four carbonyl oxygen atoms arranged in a near-perfect cube.[1]

Valinomycin (**3**), a cyclic dodecadepsipeptide composed of alternating D-valine, L-lactic acid, L-valine and D-α-hydroxyisovaleric acid residues, shows high selectivity for potassium ions. X-Ray crystallographic studies show that the metal ion lies at the centre of the molecule and is octahedrally coordinated by the carbonyl oxygens of the ester groups. The structures of the sodium and barium complexes of valinomycin as well as the uncomplexed molecule have also been determined, but these are quite different from the K^+ complex.[2]

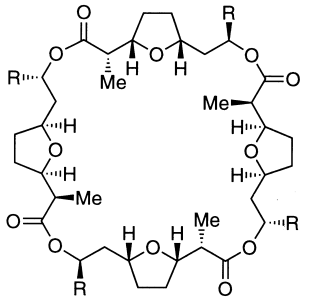

1, R = Me
2, R = Et

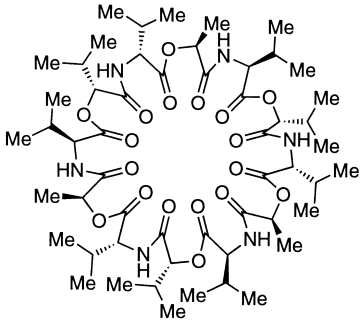

3

Enniatin B (**4**), a fungal antibiotic produced by *Fusarium orthoceras*, is a cyclohexadepsipeptide composed of alternating L-*N*-methylvalines and D-hydroxyisovaleric acid residues. Its chemical properties as well as its ion selectivities have been extensively studied.[3] The crystal structure of uncomplexed enniatin B has all the isopropyl groups

Keywords: polycyclic aliphatic compounds; macrocycles; ionophores; theoretical studies.

* Corresponding author. Present address: School of Pharmacy, The University of Queensland, Brisbane, QLD 4072, Australia; e-mail: r.mcgeary@mailbox.uq.edu.au

0040–4020/00/$ - see front matter
PII: S0040-4020(00)00724-9

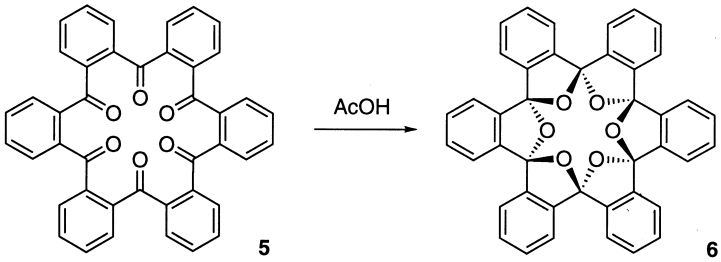

Scheme 1.

oriented pseudo-equatorially, with the six carbonyls pointing inwards and adopting alternating up–down configurations, and the carbonyl oxygens defining an approximate octahedral geometry.[4] The KI complex of enniatin B was investigated by crystallographic methods in 1969,[5] but because of the poor quality of the crystals it could not be decided whether the cations occupy the centres of the molecules, or whether they sit between them. The latter situation is consistent with observations that in solution 1:1 and 2:1 sandwich-type enniatin B:metal ion complexes exist in equilibrium.[6] In contrast to valinomycin, the enniatins do not have pronounced cation selectivity. The order of binding is $K^+ > Rb^+ > Na^+ \sim Cs^+ > NH_4^+ > Li^+$. The structurally related beauvericin has been crystallised as its barium picrate salt. In this complex the Ba^{2+} ions lie on the outside of the beauvericin ionophore ('*exo*' geometry) and coordinate to three of its carbonyl oxygens, with the other metal coordination sites being occupied by picrate anions.[7] A similar sandwich binding of Rb^+ is observed in the crystal structure of the complex with a stereoisomer of enniatin B.[8]

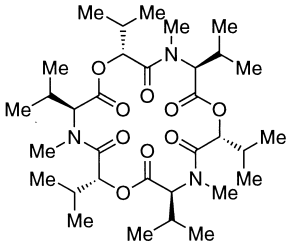

4

Recently Lee et al. reported the facile, acid-catalysed rearrangement of cyclic polyketones (e.g. **5**) (Scheme 1). The products, trivially named *starands*, have been characterised by spectroscopic, crystallographic and theoretical studies.[9–14] The six oxygen atoms of [1_6]starand (**6**) define a near-spherical cavity of diameter 1.02 Å, while its larger homologue, [1_8]starand, possesses a cavity of diameter 2.43 Å.[10] The metal binding properties of these molecules have been investigated, with [1_6]starand showing selectivity for Li^+ binding, and [1_8]starand showing strongest affinity for K^+ in methanol solution.[11,13]

A similar rearrangement of poly-1,4-diketones (**7**) to polyspiroacetals (**8**) has been reported for alternating copolymers of carbon monoxide and 1-alkenes (Scheme 2),[15] and we have recently reported on cyclic peptides and their *peptidostarand* valence tautomers.[16]

In this paper we consider the potential for cyclic polyesters, such as **9**, to undergo analogous rearrangements to give macrocyclic polyorthoesters (**10**), with carbon and oxygen atom rehybridisation from sp^2 to sp^3 centres. These molecules are of interest because of the ease with which cyclic polyesters can be synthesised,[17–19] their structural relationships to a number of naturally occurring ionophores, and the possible metal-binding properties of these molecules. This paper describes our ab initio molecular orbital calculations on the polylactone (**9**), the polyorthoester (**10**), their higher homologues **11** and **12**, and a number of metal complexes of **9** and **10** with the lighter metal ions.

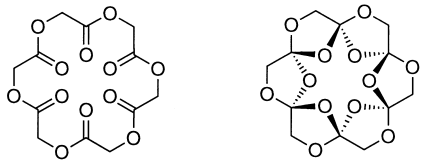

9 10

Results

Cyclic hexamer of glycolic acid

Lactone (**9**), the cyclic hexamer of glycolic acid, was subjected to an exhaustive Monte Carlo conformational search using the MM2 force field, as implemented on MacroModel, v. 4.0.[20] The coordinates of the lowest energy conformer found were then used as input for a full geometry optimisation using the 3-21G** basis set (HF/3-21G**), as implemented on GAUSSIAN 94,[21] and the optimised coordinates were then used as input for an unrestrained geometry

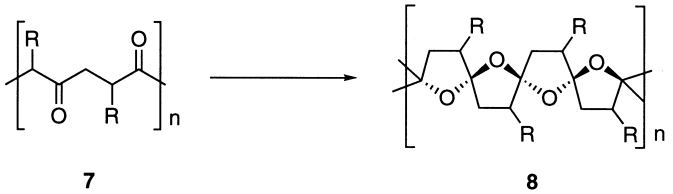

7 8

Scheme 2.

Table 1. Relative energies of the cyclic polylactone (**9**) and the cyclic polyorthoester (**10**) at various levels of theory

Molecule	HF/3-21G** (kcal/mol)	HF/6-31G* (kcal/mol)[a]	MP2//HF/6-31G* (kcal/mol)
Polylactone **9**	0	0	0
Polyorthoester **10**	4.7	44.4	37.4

[a] When unscaled zero-point corrections were taken into account, the energy difference between **9** and **10** was 49.8 kcal/mol.

optimisation on GAUSSIAN 94, using the 6-31G* basis set (HF/6-31G*). A frequency calculation on this optimised structure found only positive values, indicating that the optimised geometry represented a local energy minimum. Finally, the 6-31G* optimised coordinates were used for a single-point MP2 calculation (MP2//HF/6-31G*) to examine the effects of electron correlation. A similar process was used to derive the structure and energy of the polyorthoester (**10**).

The results of these calculations are shown in Table 1. The difference in energies calculated for **9** and **10**, at the HF/3-21G** level, was only 4.7 kcal/mol. Calculations performed at the HF/6-31G* level again gave **9** as the most stable valence tautomer, but this time by 44.4 kcal/mol. The large discrepancy between the calculations at these two levels of theory prompted us to perform single point Møller–Plesset second-order perturbation (MP2) calculations on **9** and **10** at the optimised HF/6-31G* geometries (MP2//HF/6-31G*). At this level of theory, **9** was again found to be much more stable than **10**, which confirms the HF/6-31G* result. Polyactone **9** has been isolated, as one of many products, from the pyrolysis of sodium chloroacetate. The identity of this material was confirmed by mass spectrometry and ^{1}H NMR spectroscopy, and the product's infrared spectrum showed clearly the presence of carbonyl bands.[22] The optimised geometries of **9** and **10** are shown in Fig. 1.

Cyclic hexalactone **9** adopts an S_6 symmetry in its optimised geometry, with alternating up–down arrangement of the carbonyls, similar to that seen in the crystal structure of enniatin B. Each ester group is in the *E* configuration. The carbonyl oxygens define two triangular planes separated by 2.57 Å, and the distances from each carbonyl oxygen to the centre of the molecule is 2.43 Å which, assuming the van der Waals radius of oxygen to be 1.40 Å,[23] gives a cavity diameter of 2.05 Å.

Cyclic polyorthoester **10** also adopts an S_6 symmetry in its optimised geometry, and the distance from the centre of the molecule to the proximal oxygen atoms is 1.85 Å, which gives a cavity diameter of 0.89 Å. This value is smaller than that calculated for [1$_6$]starand (**6**) (0.97 Å).[24] The parallel triangular planes defined by the interior oxygen atoms of **10** are separated by 1.56 Å.

Cyclic octamer of glycolic acid

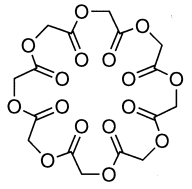

11

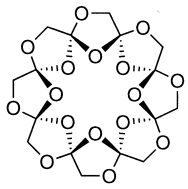

12

The lowest energy conformation of polylactone (**11**), the cyclic octamer of glycolic acid, was determined using the Monte Carlo conformational searching routine on MacroModel, employing the MM2 force field. As in the case of polylactone (**9**), the lowest energy conformation found for **11** was used as input coordinates for full optimisation at the HF/3-21G** level of theory. These optimised coordinates were then used as input for full optimisation at the HF/6-31G* level of theory. A similar procedure was used to determine the structure and energy of the cyclic polyorthoester (**12**).

The results of these calculations are shown in Table 2. The

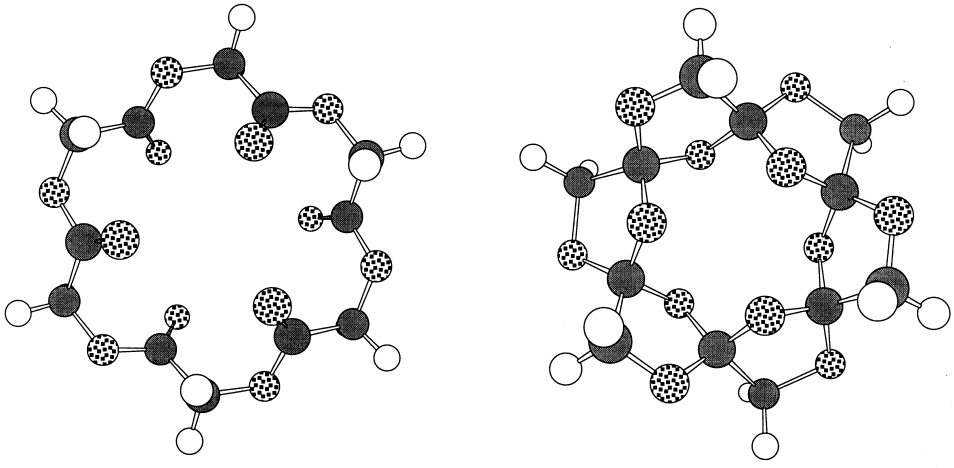

Figure 1. Optimised geometries of the cyclic hexalactone (**9**) (left), and the cyclic polyorthoester (**10**) (right).

Table 2. Relative energies of the cyclic polylactone (**11**) and the cyclic polyorthoester (**12**) at three levels of theory

Molecule	HF/3-21G** (kcal/mol)	HF/6-31G* (kcal/mol)	MP2//HF/6-31G* (kcal/mol)
Polylactone **11**	0	0	0
Polyorthoester **12**	13.0	56.5	50.5

difference in energy between **11** and **12** was calculated to be only 13.0 kcal/mol at the HF/3-21G** level of theory but, as in the case of **9** and **10**, the calculated energy difference between **11** and **12** was substantially larger at the HF/6-31G* level of theory (56.5 kcal/mol). Because of this discrepancy we again performed single point MP2 calculations on **11** and **12**, and these results (50.5 kcal/mol energy difference) were comparable with the HF/6-31G* results. The optimised geometries for these species are shown in Fig. 2.

Complexation of 9 and 10 with Metal Ions

Because we were interested in the potential of these compounds to act as ionophores, we examined the metal binding abilities of **9** and **10** with the cations Li^+, Na^+, K^+, Mg^{2+}, Be^{2+}, B^{3+} and Al^{3+}. The structures of **9** and **10** (Fig. 1) reveal that both these species are preorganised to bind metal ions, and that two modes of metal ion binding can be conceived. Hexalactone **9**, with its alternating up–down arrangement of carbonyl groups, can clearly participate as a tridentate ligand for a metal ion with the metal sitting above the plane of the molecule and along the C_3 axis, coordinating to the three closest carbonyl oxygen atoms ('exohedral binding'). Alternatively, the metal could be enclosed within the cavity of the polylactone, coordinating all six of the carbonyl atoms octahedrally (endohedral binding). These modes of binding are illustrated in Fig. 3.

A similar situation exists with polyorthoester (**10**). Again, a tripodal binding mode is possible if the metal ion sits above the molecule on the C_3 axis (exohedral binding) and, again, the metal ion could alternatively be positioned within the cavity, coordinating to six oxygen atoms (endohedral binding). These binding modes are shown in Fig. 4.

In examining the potential for these macrocycles to complex metal ions, the same general method was followed for optimising the geometries of all the metal complexes of **9** and **10**. In the case of the exohedral complexes of these macrocycles, the input coordinates were the previously optimised geometries of **9** or **10**, with the metal ions places along the C_3 axis at a distance slightly further away from the macrocycle than would be expected to be optimum. The resulting complex was first fully optimised using the HF/3-21G** basis set, and the resulting geometry was then used as starting coordinates for full optimisation using the HF/6-31G* basis set. An analogous method was used for the endohedral complexes of **9** and **10**, except that the metal ions were initially placed at the centres of the macrocycles.

Group IA Metals

Lithium

Lactone *endo*. The cavity defined by the carbonyl oxygen atoms of uncomplexed **9** has a diameter of 2.05 Å. With a Li^+ ion complexed at the centre of the molecule (*endo* complex) the oxygen atoms are displaced significantly inwards, such that the cavity now has a diameter of 1.51 Å, and the two triangular planes defined by the carbonyl oxygens now lie 2.15 Å above and below the Li^+ ion. The binding energy of Li^+ within the cavity of **9** is 104 kcal/mol.

Lactone *exo*. In the case of Li^+ binding in an *exo* manner to the lactone **9**, the optimised geometry has the metal ion lying on the C_3 axis at a distance of 1.89 Å from each of the three oxygen atoms coordinating it, but lying only 0.16 Å above the plane defined by those oxygen atoms. Binding of the Li^+ ion has the effect of slightly flattening the ligand. Whereas in the uncomplexed **9** the triangular

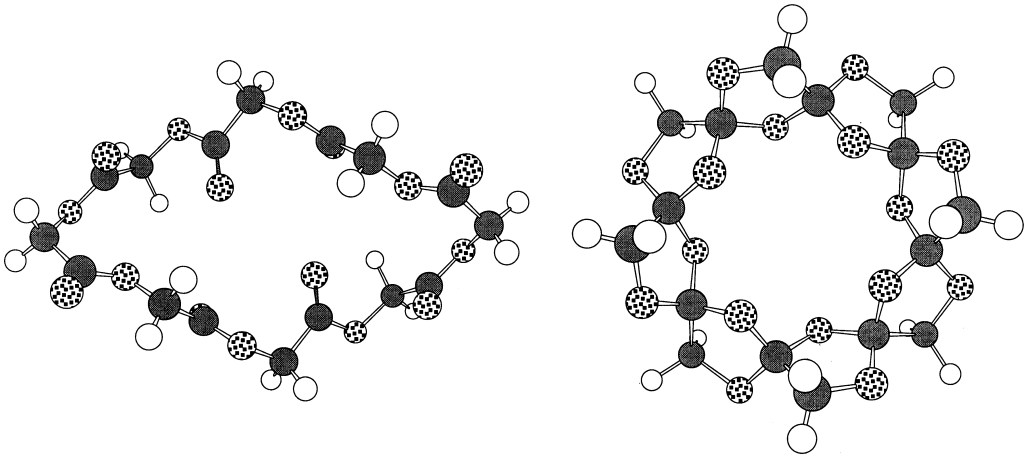

Figure 2. Optimised geometries of the cyclic octalactone (**11**) (left), and the cyclic polyorthoester (**12**) (right).

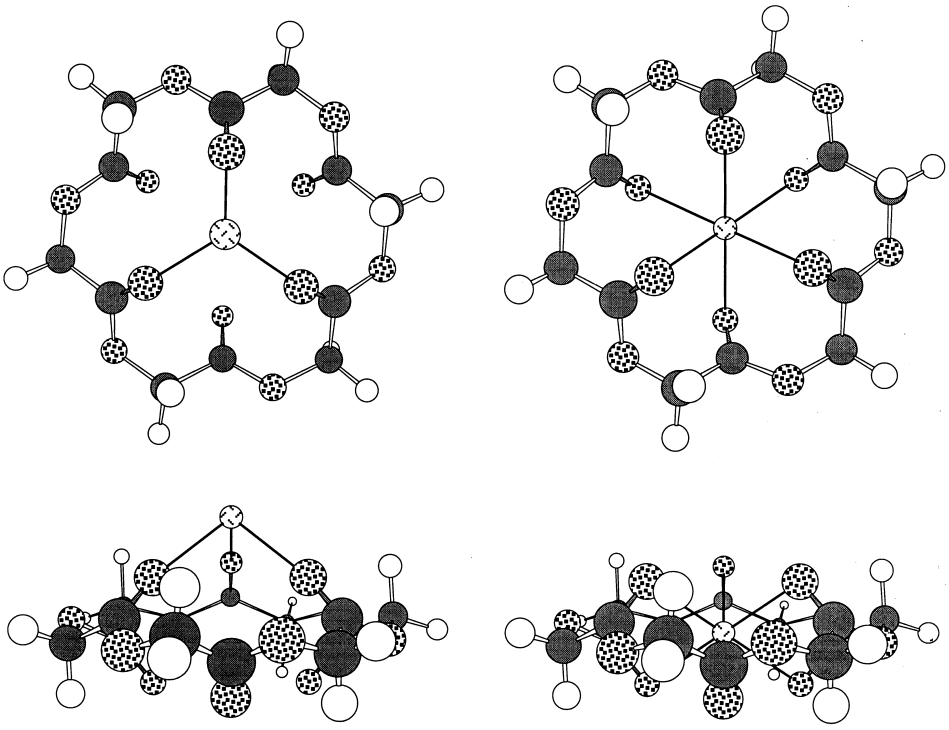

Figure 3. Possible modes of binding of polylactone (**9**) with a metal ion. Exohedral binding is shown at left, and the endohedral binding mode is displayed at right.

planes defined by the carbonyl oxygens were separated by 2.57 Å, the *exo*-Li^+ complex has this distance reduced to 2.36 Å. The binding energy for Li^+ with **9** in this *exo* manner is 103 kcal/mol, almost identical to that obtained by *endo* binding.

Orthoester *endo*. The cavity defined by the ether oxygens of uncomplexed **10** is 0.89 Å in diameter. While this distance appears to be too small to fit most metals, we find that when Li^+ is placed at the origin, the optimised geometry of the resulting complex is only marginally

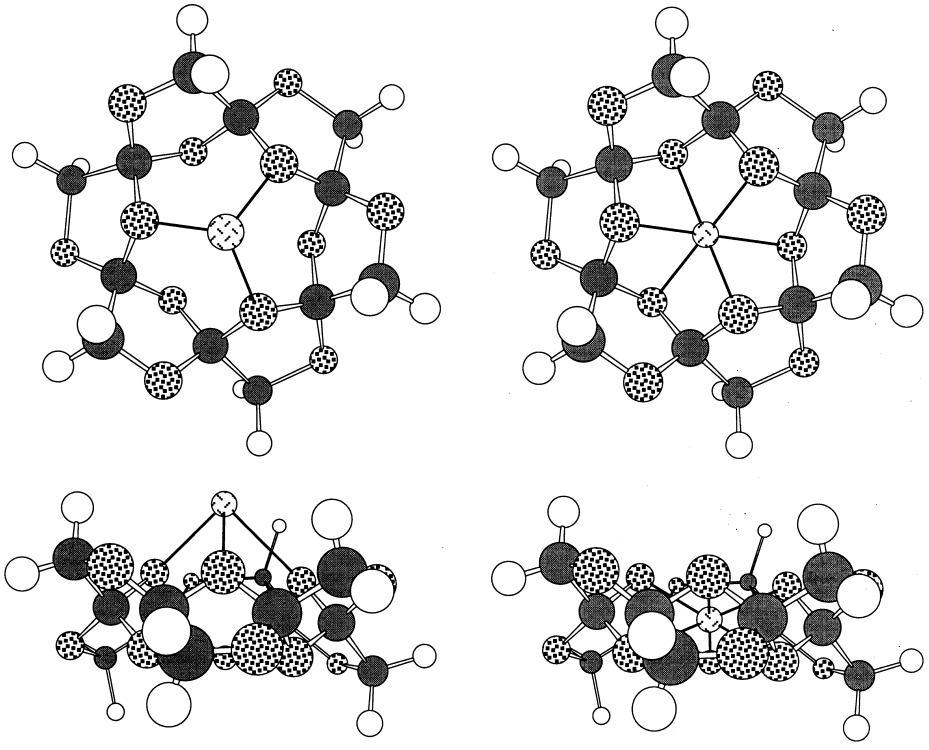

Figure 4. Possible modes of binding of polyorthoester (**10**) with a metal ion. Exohedral binding is shown at left, and the endohedral binding mode is displayed at right.

distorted from the original structure of **10**. Specifically, while the six oxygen atoms are displaced slightly outwards from the metal ion such that the cavity diameter of the *endo*-Li^+ complex of **10** is now expanded to 0.91 Å, the distance separating the triangular planes defining the coordinating oxygen atoms is *reduced* to 1.54 Å, slightly less than in the case of **10** itself (1.56 Å). The binding energy for Li^+ with **10** in this *endo* manner is 50 kcal/mol.

Orthoester *exo*. In the case of Li^+ binding in an *exo* manner to **10**, the optimised geometry has the metal ion lying on the C_3 axis at a distance of 1.94 Å from each of the three oxygen atoms coordinating it, and lying 1.02 Å above the plane defined by those oxygen atoms. The distance between the two planes of oxygen atoms in the *exo* complex is 1.56 Å, the same as in **10**. The binding energy for Li^+ with **10** in the *exo* manner is 72 kcal/mol.

Sodium

Lactone *endo*. With a Na^+ ion complexed at the centre of lactone **9** (*endo* complex) the carbonyl oxygen atoms are displaced inwards significantly, such that the cavity now has a diameter of 1.79 Å (cf. 2.05 Å for uncomplexed **9**), and the two triangular planes defined by the carbonyl oxygens now lie 2.31 Å above and below the Na^+ ion. The binding energy for Na^+ with **9** (*endo*) is 77 kcal/mol.

Lactone *exo*. In the case of Na^+ binding in an *exo* manner to the lactone **9**, the optimised geometry has the metal ion lying on the C_3 axis at a distance of 2.21 Å from each of the three oxygen atoms coordinating it, and lying 0.77 Å above the plane defined by those oxygen atoms. As was observed in the case of Li^+ binding in an *exo* mode to **9**, *exo* binding of the Na^+ ion has the effect of slightly flattening the ligand. The binding energy for Na^+ with **9** in this *exo* manner is 78 kcal/mol and, as is the case with Li^+, the binding energy is almost exactly the same for the *exo* and the *endo* modes of binding.

Orthoester *endo*. As expected, when Na^+ is placed at the origin of **10**, the optimised geometry of the resulting complex is significantly distorted from the original structure of **10**. The six coordinating oxygen atoms are displaced outwards from the metal ion such that the cavity diameter of the *endo*-Na^+ complex of **10** is now expanded to 1.13 Å, and the metal–oxygen distances are now a very low 1.96 Å. However, the distance separating the triangular planes defining the oxygen atoms coordinating to the metal is now 1.56 Å, exactly the same as in the case of **10** itself. The binding energy for Na^+ with **10** in this *endo* manner is −50 kcal/mol, i.e. endothermic.

Orthoester *exo*. For Na^+ binding *exo* to **10**, the optimised geometry has the metal ion lying on the C_3 axis at a distance of 2.31 Å from each of the three oxygen atoms coordinating it, and lying 1.59 Å above the plane defined by those oxygen atoms. The binding energy for Na^+ with **10** in the *exo* manner is 50 kcal/mol.

Potassium[†]

Lactone *endo*. Hexalactone (**9**) appears to accommodate an *endo* K^+ ion very well. The coordinating carbonyl oxygen atoms are displaced outwards significantly from the starting structure (**9**), such that the cavity now has a diameter of 2.26 Å, and the two triangular planes defined by the carbonyl oxygens now lie 1.29 Å above and below the K^+ ion. The distance between the metal ion and the carbonyl oxygen atoms is 2.53 Å, in the normal range for a K–O bond. The binding energy for K^+ with **9** (*endo*) is 48 kcal/mol.

Lactone *exo*. *exo* Binding of K^+ to **9** leads to the optimised geometry having the metal ion lying on the C_3 axis at a distance of 2.55 Å from each of the three oxygen atoms coordinating it, and lying 1.39 Å above the plane defined by those oxygen atoms. The binding energy for K^+ with **9** in this *exo* manner is 71 kcal/mol, significantly higher than for the case of *endo* binding.

Orthoester *endo*. The cavity defined by the ether oxygens of **10** (0.89 Å in diameter) is too small to accommodate the potassium ion without severe distortion of the ligand. In the optimised geometry the six coordinating oxygen atoms are displaced significantly outwards from the metal ion such that the cavity diameter of the *endo*-K^+ complex of **10** is now expanded to 1.53 Å, giving K–O bond lengths of only 2.16 Å, indicating severe strain in the complex. The binding energy for K^+ with **10** in this *endo* manner is −178 kcal/mol, i.e. highly endothermic.

Orthoester *exo*. For K^+ binding in an *exo* manner to **10**, the optimised geometry has the metal ion lying on the C_3 axis at a distance of 2.62 Å from each of the three oxygen atoms coordinating it, and lying 1.98 Å above the plane defined by those oxygen atoms. The binding energy for K^+ with **10** in the *exo* manner is 57 kcal/mol.

Group IIA Metals

Beryllium

Lactone *endo*. With a Be^{2+} ion complexed at the centre of **9** (*endo* complex) the oxygen atoms are displaced significantly inwards, such that the cavity now has a diameter of only 1.07 Å. The distance between the metal ion and the carbonyl oxygens is 1.94 Å, somewhat longer than optimum, and the two triangular planes defined by the carbonyl oxygens now lie 0.96 Å above and below the Be^{2+} ion. The binding energy for Be^{2+} with **9** (*endo*) is 380 kcal/mol.

Lactone *exo*. For Be^{2+} binding in an *exo* manner to the lactone **9**, the optimised geometry has the metal ion lying on the C_3 axis, and adopting a trigonal geometry, such that the metal ion lies almost in the plane of the three coordinating carbonyl oxygens. In fact, the Be^{2+} ion is offset by 0.07 Å *towards* the centre of the molecule. The Be–O distance is 1.56 Å. Binding of the Be^{2+} ion has the effect of significantly flattening the ligand. Whereas in the uncomplexed cyclic lactone **9** the triangular planes defined by the carbonyl oxygens are separated by 2.57 Å, the *exo*-Be^{2+}

[†] All calculations involving potassium were done using the 3-21G** basis set.

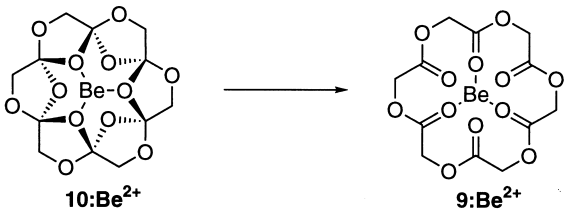

Scheme 3.

complex has this distance reduced to 2.18 Å. The binding energy for Be^{2+} with **9** in this *exo* manner is 444 kcal/mol, significantly higher than the *endo* case.

Orthoester *endo*. We find that when Be^{2+} is placed within the cavity of **10**, the six coordinating oxygen atoms are displaced *inwards* towards the metal ion such that the cavity diameter of the *endo*-Be^{2+} complex of **10** is now reduced to only 0.75 Å (cf. 0.89 Å for **10**), giving a Be–O bond length of 1.78 Å. The binding energy for Be^{2+} with **10** in this *endo* manner is 328 kcal/mol.

Orthoester *exo*. When the Be^{2+} ion was initially placed *exo* to the macrocycle **10**, and the whole complex was then optimised, a most unusual result was obtained. The resulting geometry was exactly that obtained for the geometry optimisation of the lactone-*exo* complex of Be^{2+}, as described above. This result was obtained regardless of the distance that the metal ion was positioned from the ligand, and the same result was also obtained regardless of whether the 3-21G** or the 6-31G* basis set was used for the geometry optimisation. It would appear that there is no stable complex of the polyorthoester **10** with a Be^{2+} positioned *exo* to it, and that such a complex would rearrange to the lactone structure, with the metal ion still positioned *exo* (Scheme 3).

Magnesium

Lactone *endo*. With a Mg^{2+} ion complexed at the centre of **9** (*endo* complex) the coordinating carbonyl oxygen atoms are displaced significantly inwards relative to the starting structure, such that the cavity now has a diameter of only 1.38 Å (cf. 2.05 Å for **9**), and the two triangular planes defined by the carbonyl oxygens now lie only 1.01 Å above and below the Mg^{2+} ion. The binding energy for Mg^{2+} with **9** (*endo*) is 293 kcal/mol. The Mg–O bond lengths are 2.09 Å.

Lactone *exo*. No stable structure could be found with the Mg^{2+} ion bound to the lactone **9** in an *exo* manner. The metal ion was initially placed along the C_3 axis at a distance of 1.90 Å from the centre of the lactone, and the resulting geometry optimised using the 3-21G** basis set. The metal ion migrated to the centre of the lactone **9**, and gave a structure and energy identical to that obtained when the metal was initially placed at the origin before geometry optimisation. The same result was obtained when the 6-31G* basis set was used directly. Again the final structure was identical to the 'lactone-*endo*' Mg^{2+} complex.

Orthoester *endo*. When Mg^{2+} is placed at the origin of **10**, the optimised geometry of the resulting complex is slightly distorted from the original structure. Specifically, the six oxygen atoms are displaced outwards such that the cavity diameter of the *endo*-Mg^{2+} complex of **10** is now increased to 1.01 Å. The binding energy for Mg^{2+} with **10** in this *endo* manner is 157 kcal/mol. The Mg–O bond lengths are 1.91 Å.

Orthoester *exo*. In the case of Mg^{2+} binding in an *exo* manner of **10**, the optimised geometry has the metal ion lying on the C_3 axis at a distance of 1.97 Å from each of the three oxygen atoms coordinating it, and lying 1.07 Å above the plane defined by those oxygen atoms. The binding energy for Mg^{2+} with **10** in the *exo* manner is 197 kcal/mol.

Group IIIB Metals

Boron

Lactone *endo*. The largest distortion of the polylactone **9** is observed when a B^{3+} ion is complexed at its centre (*endo* complex). The oxygen atoms are displaced significantly inwards, such that the cavity now has a diameter of only 0.67 Å (cf. 2.05 Å in uncomplexed **9**). The distance between the contiguous (on opposite faces) carbonyl oxygen atoms, 2.38 Å, is now shorter than then the sum of their van der Waals radii, and the two triangular planes defined by the carbonyl oxygens now lie only 0.94 Å above and below the B^{3+} ion. The binding energy for B^{3+} with **9** (*endo*) is 969 kcal/mol.

Lactone *exo*. No stable symmetrical structure could be located with the lactone **9** binding B^{3+} in an *exo* manner. When, using the 3-21G** basis set, the metal ion was initially placed along the C_3 axis at a distance of 1.90 Å from the centre of the complex, the optimised geometry had a very unsymmetrical shape with the metal ion coordinating to only one carbonyl oxygen (Fig. 5). The same result was obtained when the process was repeated using the 6-31G* basis set directly. The only B–O distance is 1.45 Å. The binding energy for B^{3+} with **9** in this *exo* manner is 819 kcal/mol.

Orthoester *endo*. No stable structure could be found with the B^{3+} ion lying at the centre of the polyorthoester ligand. When the metal ion was initially placed at the centre of the ligand and the geometry was optimised, using either the 3-21G** or 6-31G* basis set, the final structure was the same as that which resulted from the 'orthoester *exo*' case (see below).

Orthoester *exo*. In the case of B^{3+} binding in an *exo* manner to **10**, the optimised geometry had a most unexpected structure. We found that three of the C–O bonds had broken, with the oxygen atoms in each case now binding to the B^{3+}, such that three dioxycarbocations were formed (**13**, Fig. 6). The boron is bound in a trigonal geometry, with the B–O bonds 1.37 Å long, and the proximal O–O distances only 2.38 Å. The boron atom lies almost exactly in the plane defined by the three proximal oxygens. The binding energy for B^{3+} with **10** in this manner is 1089 kcal/mol, significantly higher than for the case of the **9**:B^{3+} complexes.

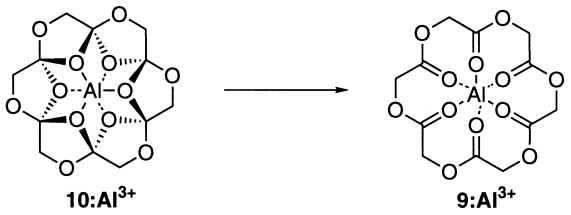

Scheme 4.

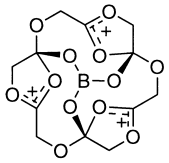

13

Aluminium

Lactone *endo*. When an Al^{3+} ion is complexed at the centre of the polylactone **9** (*endo* complex), the oxygen atoms are displaced significantly inwards from their starting positions, such that the cavity of the macrocycle now has a diameter of only 1.07 Å, with Al–O distances of 1.94 Å. The binding energy of Al^{3+} with **9** (*endo*) is 691 kcal/mol.

Lactone *exo*. No stable structure could be located with the lactone **9** binding Al^{3+} in an *exo* manner. When the metal ion was initially placed along the C_3 axis at a distance of 1.90 Å from the centre of the complex, the metal ion migrated during optimisation to the centre of the molecule and attained an optimised geometry identical to the 'lactone *endo*' case obtained above. The same result was obtained whether the 3-21G** or the 6-31G* basis sets were used.

Orthoester *endo*. When the metal ion was initially placed at the centre of the ligand and the geometry was optimised, using either the 3-21G** or 6-31G* basis set, we were surprised to find that the final structure was identical to the 'lactone *endo*' one obtained above. Thus, it appeared that the polyorthoester structure in **10** was unstable with an Al^{3+} placed at the origin, and rearranged to the polylactone form with the metal ion at the centre of the complex (Scheme 4). This is analogous to the rearrangement which occurred when Be^{2+} was placed *exo* to **10** (Scheme 3).

Orthoester *exo*. In the case of Al^{3+} binding in an *exo* manner to **10**, the optimised geometry using the 3-21G** basis set was again found to be identical to the 'lactone *endo*' structure calculated above. That is, the metal ion had migrated to the centre of the complex, and the bonds had rearranged to the polylactone structure. However when the 6-31G* basis set was used directly, we obtained a stable structure analogous to the boron orthoester *exo* structure obtained above, i.e. with the tricarbocation structure and the Al^{3+} lying nearly in the plane of the three oxygen atoms coordinating it (**14**). The aluminium ion is bound in a trigonal geometry, with the Al–O bonds 1.73 Å long, and the distances between the proximal oxygens 2.99 Å. The aluminium atom lies very slightly above the plane defined by the three proximal oxygens (0.15 Å). The

Table 3. Summary of the energies and geometries of **9** and **10**, and their complexes with metal ions

Molecule	Symmetry	Binding energy (kcal/mol)	Cavity diameter (Å)	Metal–oxygen distance (Å)
9	S_6	–	2.05	–
9-Li^+ (*endo*)	S_6	104.4	1.51	2.156
9-Li^+ (*exo*)	C_3	103.1	–	1.893
9-Na^+ (*endo*)	S_6	77.3	1.79	2.293
9-Na^+ (*exo*)	C_3	77.7	–	2.209
9-K^+ (*endo*)	S_6	47.9	2.26	2.528
9-K^+ (*exo*)	C_3	71.0	–	2.545
9-Be^{2+} (*endo*)	S_6	380.3	1.07	1.935
9-Be^{2+} (*exo*)	C_3	443.9	–	1.561
9-Mg^{2+} (*endo*)	S_6	293.3	1.38	2.091
9-Mg^{2+} (*exo*)	–	–	–	–
9-B^{3+} (*endo*)	S_6	968.8	0.67	1.731
9-B^{3+} (*exo*)	C_1	819.5	–	
9-Al^{3+} (*endo*)	S_6	690.9	1.07	1.937
9-Al^{3+} (*exo*)	–	–	–	–
10	S_6	–	0.89	
10-Li^+ (*endo*)	S_6	49.5	0.91	1.856
10-Li^+ (*exo*)	C_3	71.8	–	1.938
10-Na^+ (*endo*)	S_6	−49.8	1.13	1.963
10-Na^+ (*exo*)	C_3	49.5	–	2.307
10-K^+ (*endo*)	S_6	−178.0	1.53	2.163
10-K^+ (*exo*)	C_3	56.9	–	2.616
10-Be^{2+} (*endo*)	S_6	328.5	0.75	1.776
10-Be^{2+} (*exo*)	–	–	–	–
10-Mg^{2+} (*endo*)	S_6	157.2	1.01	1.906
10-Mg^{2+} (*exo*)	C_3	196.5	–	1.974
10-B^{3+} (*endo*)[a]	C_3	1089.3	–	1.374
10-B^{3+} (*exo*)[a]	C_3	1089.3	–	1.374
10-Al^{3+} (*endo*)	C_3	–	–	–
10-Al^{3+} (*exo*)[a]	C_3	643.1	–	1.731

[a] See text.

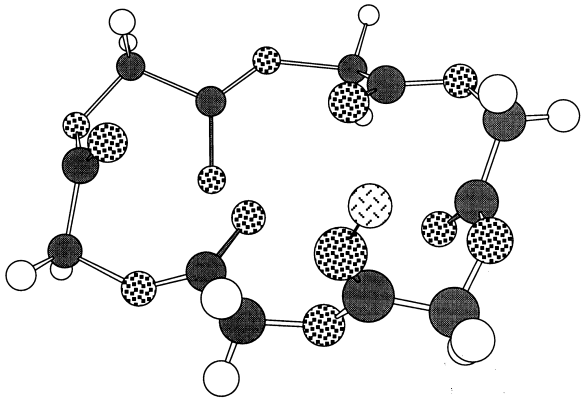

Figure 5. Optimised geometry of the complex arising when a B^{3+} ion was placed *exo* along C_3 axis of polylactone (**9**).

binding energy for Al^{3+} with **10** in this manner is 643 kcal/mol.

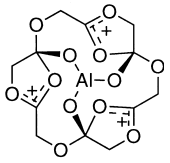

14

These results are summarised in Table 3.

Discussion

Our calculations show that the polylactone (**9**) is significantly lower in energy than its polyorthoester valence tautomer (**10**) and, similarly, that polylactone (**11**) is lower in energy than its valence tautomer (**12**). This is in contrast to the analogous starands (**6**) which are more stable than their polyketone isomers (**5**), and probably results from the increased importance of delocalisation energy of the ester groups in **9** and **11**, compared with the unsaturated ketone units in **5**. In the case of peptidostarands, these compounds were calculated to be much less stable than their isomeric cyclic peptides, and this was attributed to the delocalisation energy of the amide bond. Indeed, it was calculated that substitution of the nitrogens in cyclic peptides with strongly electron-withdrawing groups led to a reversal of the relative stabilities, such that the peptidostarand valence tautomers were more stable.[16]

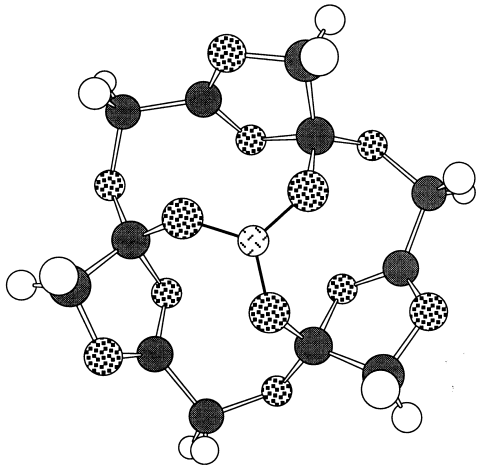

Figure 6. Optimised geometry of the unexpected complex arising when a B^{3+} ion was placed either *endo* or *exo* along C_3 axis of polyorthoester (**10**).

The polylactone **9** was flexible enough to accommodate all the metal ions examined and to bind exothermally with them. The binding of Li^+ to **9** was calculated to be almost equally exothermic for both the *endo* and *exo* modes, and this was also seen in the case of Na^+. There was a preference for K^+ and Be^{2+} to bind to **9** exohedrally, but no stable structures for *exo*-binding of Mg^{2+} or Al^{3+} to **9** were found; in both cases these ions migrated to the centre of **9** during geometry optimisation. The preference for exohedral binding of K^+ of **9** would support the sandwich model of K^+ binding for the enniantins.[6] There was a strong preference found for B^{3+} to bind **9** endohedrally, leading to a complex markedly distorted from the uncomplexed structure. Attempts to optimise the *exo*-B^{3+} complex of **9** led to an unsymmetrical structure (Fig. 5) in which the metal ion was coordinated to only one carbonyl oxygen.

Of the metal ions examined for binding endohedrally within the cavity of **10**, only the complexation of Na^+ and K^+ was unfavourable, presumably due to their large size and severe strain in the resulting complexes (for both B^{3+} and Al^{3+} these systems rearranged). There was a moderate preference for both Li^+ and Mg^{2+} to bind exohedrally to **10**, but while the cavity diameter in uncomplexed **10** is calculated to be 0.89 Å, both Li^+ and Mg^{2+} (ionic diameters 1.18 and 0.98 Å, respectively[23]) were still able to fit comfortably, i.e. with minimal distortion of **10**. This type of phenomena has been observed in the case of spherand (**15**), which is capable of complexing Na^+ endohedrally, even though its cavity diameter (1.62 Å) is significantly smaller than the ionic diameter of Na^+ (1.94 Å).[25] This was rationalised as a relief of strain caused by oxygen–oxygen interactions in the uncomplexed ligand.

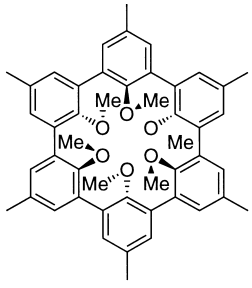

15

In several of the cases examined, the structures consisting of a metal ion bound exohedrally to polyorthoester (**10**) do not appear to be minima on the energy hypersurface. We found for example that while Be^{2+} fits comfortably within the cavity of **10**, the structure with Be^{2+} bound exohedrally rearranged during the geometry optimisation to the same arrangement as was found for Be^{2+} binding exohedrally to **9**. A similar rearrangement was seen for the endohedral complex of **10** with Al^{3+}—again the orthoester structure

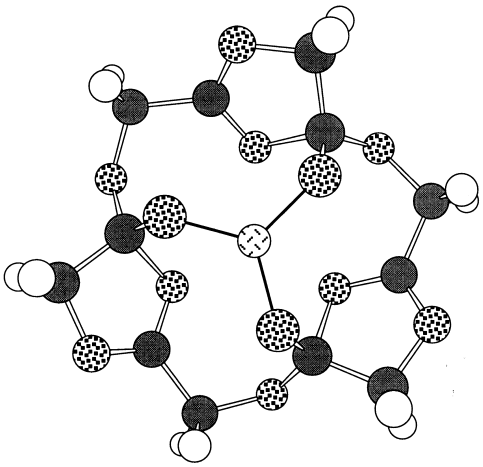

Figure 7. Optimised geometry of the complex arising when an Al^{3+} ion was placed *exo* along C_3 axis of polyorthoester (**10**).

rearranged to the polylactone to give the same structure as was obtained for Al^{3+} binding endohedrally to **9**.

The most surprising result was obtained in the case of B^{3+} binding to **10**, either endohedrally or exohedrally. We found that a new type of complex was formed, the result of the breaking of three B–O bonds to give three oxygen-stabilised carbocations (Fig. 6). An analogous structure was obtained by geometry optimisation of the exohedral Al^{3+} complex of **10** (Fig. 7).

It was of interest to examine the structures and energies of 2:1 ligand:metal complexes, analogous to the sandwich complexes described for enniatin B (**4**) and its stereoisomers.[4–6] Such complexes could form between a metal and two molecules of **9** and/or **10**, each binding to the metal in an *exo* manner. Such calculations were attempted at the HF/3-21G** level of theory but, due to the large number of heavy atoms, these calculations exceeded the computer resources available to us (a Silicon Graphics ORIGIN 2000 with 64 CPUs). For Gaussian molecular orbital calculations computer resource requirements (CPU time and memory usage) increase exponentially, approximately proportional to the number of basis functions to the power of 3.5.[26]

Conclusion

The geometries and energies of the cyclic hexamer of glycolic acid (**9**) and its cyclic polyorthoester valence tautomer (**10**) have been studied by ab initio molecular orbital calculations. At the MP2//HF/6-31G* level of theory we find that the cyclic polyester isomer (**9**) is more stable than **10** by 37.4 kcal/mol, a much greater difference than that obtained from HF/3-21G** calculations (4.7 kcal/mol).

The cyclic octamer of glycolic acid (**11**) and its cyclic orthoester valence tautomer (**12**) have also been studied by ab initio molecular orbital calculations, and here too we find that the cyclic polyester is more stable than its valence tautomer, in this case by 50.5 kcal/mol at the MP2//HF/6-31G* level of theory.

The metal-binding properties of **9** and **10** with Li^+, Na^+, K^+, Be^{2+}, Mg^{2+}, B^{3+} and Al^{3+} have been investigated. All the group IA metals bound more strongly to the polylactone **9** than to **10**. For the IIA metals, Be^{2+} binds preferably to **9** rather than **10**, in either the *endo* or *exo* modes, and Mg^{2+} also binds in an *endo* manner to **9** more strongly than to **10**. In the case of the IIIB metals, B^{3+} binds more favourably with the rearranged tricarbocation (**13**, Fig. 6) than it does with **9**. However Al^{3+} binds more strongly with **9** than with the rearranged tricarbocation (**14**).

Supplementary material

A listing of energies and Cartesian coordinates of all optimised geometries described may be obtained from the corresponding author.

Acknowledgements

We thank Dr Ian Bytheway for helpful discussions. A generous allocation of supercomputer time at the High Performance Computing Facility at The University of Queensland is gratefully acknowledged. This research was supported by a University of Queensland Foundation Award (to R. P. M.).

References

1. Dobler, M. *Ionophores and Their Structures*; Wiley: New York, 1981.
2. Duax, W. L.; Griffin, J. F.; Langs, D. A.; Smith, G. D.; Grochulski, P.; Pletnev, V.; Ivanov, V. *Biopolymers* **1996**, *40*, 141–155.
3. Ovchinnikov, Y. A.; Ivanov, V. T. The cyclic peptides: structure, conformation, and function. In *The Peptides*, 3rd ed.; Neurath, H., Hill, R. C., Eds.; Academic Press: New York, 1982; Vol. 5, pp 365–373 (also pp 516–529).
4. Kratky, C.; Dobler, M. *Helv. Chim. Acta.* **1985**, *68*, 1798–1803.
5. Dobler, M.; Dunitz, J. D.; Krajewski, J. *J. Mol. Biol.* **1969**, *42*, 603.
6. Ivanov, V. T.; Evstratov, A. V.; Sumskaja, L. V.; Melnik, E. I.; Chumburidze, T. S.; Portnova, S. L.; Balashova, T. A.; Ovchinnikov, Y. A. *FEBS Lett.* **1973**, *36*, 65.
7. Braden, B.; Hamilton, J. A.; Sabesan, M. N.; Steinrauf, L. K. *J. Am. Chem. Soc.* **1980**, *102*, 2704–2709.
8. Tishchenko, G. N.; Karimov, Z. *Kristallografiya* **1978**, *23*, 729.
9. Lee, W. Y.; Park, C. H.; Kim, S. *J. Am. Chem. Soc.* **1993**, *115*, 1184–1185.
10. Lee, W. Y.; Park, C. H. *J. Org. Chem.* **1993**, *58*, 7149–7157.
11. Lee, W. Y. *Synlett* **1994**, 765–776.
12. Cho, S. J.; Hwang, H. S.; Park, J. M.; Oh, K. S.; Kim, K. S. *J. Am. Chem. Soc.* **1996**, *118*, 485–486.
13. Hwang, S.; Lee, H. L.; Ryu, G. H.; Jang, Y. H.; Lee, S. B.; Lee, W. Y.; Hong, J.-I.; Chung, D. S. *J. Org. Chem.* **2000**, *65*, 536–542.
14. Cho, S. J.; Kollman, P. A. *J. Org. Chem.* **1999**, *64*, 5787–5793.
15. Di Benedetto, S.; Consiglio, G. *Helv. Chim. Acta* **1997**, *80*, 2204–2214.
16. McGeary, R. P.; Bruget, D. N. *Tetrahedron Lett.* **1999**, *40*, 3041–3044.
17. Kuisle, O.; Quinoa, E.; Riguera, R. *J. Org. Chem.* **1999**, *64*, 8063–8075.

18. Kuisle, O.; Quinoa, E.; Riguera, R. *Tetrahedron Lett.* **1999**, *40*, 1203–1206.
19. Lee, B. H. *Tetrahedron Lett.* **1997**, *38*, 757–760.
20. Mohamadi, F.; Richards, N. G. J.; Guida, W. C.; Liskamp, E.; Lipton, C.; Caulfield, C.; Chang, G.; Hendrickson, T.; Still, W. C. *J. Comp. Chem.* **1990**, *11*, 440.
21. Frisch, M. J.; Trucks, G. W.; Schlegel, H. B.; Gill, P. M. W.; Johnson, B. G.; Robb, M. A.; Cheeseman, J. R.; Keith, T. A.; Petersson, G. A.; Montgomery, J.A.; Raghavachari, K.; Al-laham, M. A.; Zakrzewski, V. G.; Ortiz, J.V.; Foresman, J. B.; Cioslowski, J.; Stefanov, B. B.; Nanayakkara, A.; Challacombe, M.; Peng, C. Y.; Ayala, P. Y.; Chan, W.; Wong, M.W.; Andres, J. L.; Replogle, E. S.; Gomperts, R.; Martin, R. L.; Fox, D. J.; Binkley, J. S.; Defrees, D. J.; Baker, J.; Stewart, J. P.; Head-Gordon, M.; Gonzalez, C.; Pople, J. A. GAUSSIAN 94 (Revisions B.2 and D.1) Gaussian, Inc., Pittsburgh, PA, 1995.
22. Dale, J.; Sevaldsen, O.; Titlestad, K. *Acta Chem. Scand. B.* **1978**, *32*, 306–312.
23. Emsley, J. *The Elements*, 2nd ed.; Oxford University Press: Oxford, 1991.
24. Cui, C.; Cho, S. J.; Kim, K. S. *J. Phys. Chem. A.* **1998**, *102*, 1119–1123.
25. Trueblood, K. N.; Knobler, C. B.; Maverick, E.; Helgeson, R. C.; Brown, S. B.; Cram, D. J. *J. Am. Chem. Soc.* **1981**, *103*, 5594–5596.
26. Foresman, J. B.; Frisch, A. *Exploring Chemistry with Electronic Structure Methods*, 2nd ed.; Gaussian, Inc: Pittsburgh, PA, 1996.